

Numerical study on the effects of obstacle shape on the SDT and DDT run-up distance in a tube

G.T. Zhang¹, Y.T. Jiang¹, M.S. Yip¹, B.J.D. Liu¹, E. Daniau², and F. Falempin³

¹DSO National Laboratories, 20 Science Park Dr. Singapore 118230,

²MBDA-F, 8 rue Le Brix, 18020 Bourges CEDEX – France

³MBDA-F, 2 rue Beranger, 92323 Châtillon CEDEX – France

1 Introduction

Deflagration-to-detonation transition (DDT) and shock-to-detonation transition (SDT) are two phenomena that are commonly used to achieve detonation in various mixtures with a minimal amount of initial energy. The addition of turbulence-enhancement devices [1]-[3] (obstacles, diaphragms, screens, Shchelkin spirals, rods, etc) inside the tube is a proven way to reduce the DDT distance, but the optimum geometry is generally a function of the combustible mixture. In order to design a compact, yet efficient way to initiate a detonation inside the main combustion chamber of a Pulsed Detonation Engine, the capability to simulate flame acceleration in a tube with a complex internal geometry is mandatory.

In support of experimental work performed within an MBDA-F – DSO collaboration, a fundamental numerical study of flame acceleration was performed by DSO. The research is aimed at enabling the efficient optimization an ignition device of a future PDE ground demonstrator and to evaluate the capability of a COTS CFD package to qualitatively predict the hydrodynamic processes in the acceleration of a flame in a tube.

This paper first gives a brief overview of the fundamental processes to be simulated, and details the sensitivity of the numerical model to variables such as mesh size, heat losses, chemical kinetics and turbulence model. The second part of the paper will present a comparison between experimental results and numerical simulations.

2 Computation hypothesis

The general process of flame acceleration leading to DDT can be summarized thus: Following a spark ignition, a flame kernel undergoes various stages of flame development, and under certain conditions, may transition into detonation. A flame kernel initially begins as a laminar flame, which, due to hydrodynamic and diffusion instabilities, rapidly transforms into a turbulent flame brush. This results in flame acceleration because of the increase in surface area of flame. In tube with regular obstacles, the turbulent flame propagation regime is self-accelerating because of the feedback mechanism between the flame velocity and the level of turbulence ahead of the flame front.

Since, for a DDT process, the flame undergoes acceleration from a slow deflagration, transitioning to a supersonic flame and then to a detonation, accurate prediction of all three flame regimes is essential to accurately predict DDT distance. The simulation of flame acceleration thus produced can be a strong function of a variety of CFD modeling parameters, including, but not limited to, the mesh size, chemical kinetics models, turbulence effects, and thermal exchange and heat losses.

(a). The effect of the mesh size:

Being a shock-induced flame, a (simulated) propagating detonation can be very sensitive to the grid size and the ability of the numerical model to accurately capture the bow shock. It was found in [4] that an extremely fine mesh of order 5×10^{-3} mm was required to capture the detailed microscopic onsets of hot spot formation and their

subsequent development into a detonation. Since the use of such a fine mesh is computationally prohibitive for simulations of DDT phenomena within a practical PDE, the dominant processes leading up to the onset of DDT will instead be captured at the macro-scale with a relatively coarser mesh in the present study. It was suggested in [5] that a mesh size of between 0.5 mm to 1.0 mm was sufficient to capture the reaction zone with thickness in the order of 5.0 mm. In the present study, grid independence studies were performed to identify the minimum requirement of grid size for the model problem of our interests. 2D CFD studies of an obstacle-laden tube with cross-sectional area of 25×25 mm and channel length of 300mm with an ethylene-air mixture were carried out. It was found as shown in Figure 1 that a mesh size of less than 0.25mm is necessary to accurately predict the detonation process in the model problem.

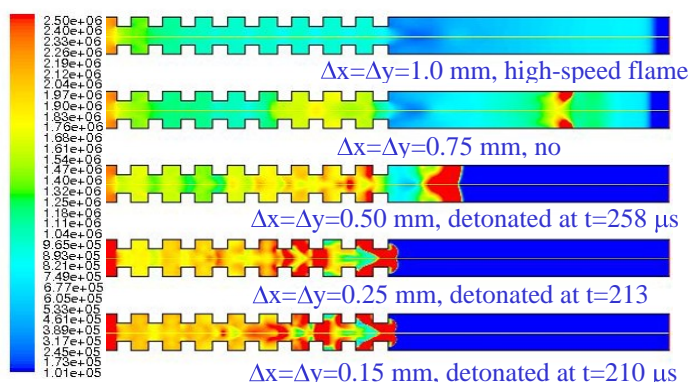


Figure 1: Grid independence study for detonation simulation: pressure contours at time instant of shock-to-detonation (if occurs) with different mesh size

(b). Kinetic model description:

Numerical modeling of the combustion process in pulse detonation engines requires an accurate representation of the interaction between fluid mechanics and chemistry, an essential component of which is the chemical kinetic reaction mechanism that describes the oxidation of the fuel [6]. Detailed mechanisms (more than 100 reaction and tens of species) are generally validated for use over a wide range of pressures, temperatures and equivalence ratios, but coupling such mechanisms with a 2D or 3D Navier – Stokes numerical scheme generally takes too much CPU time to be practical, and thus reduced mechanisms are favored. The term “reduced mechanism” is used in a broad sense, and encompasses mechanisms which are based on mathematical models with a certain degree of empiricism and fitting.

Several reduced kinetic descriptions have been introduced for hydrocarbon-air detonation studies [7]-[9]. The main difficulty for those models is to be able to take into account the structure and stability of a detonation. In the present study, 2-step kinetic mechanisms by Varatharajan et al. [7] were implemented as user-defined functions (UDF) in FLUENT. These 2-step mechanisms are attractive as they are able to reproduce the two distinct phenomena in a ZND detonation wave: 1) An iso-thermal induction period immediately behind the incident shock, and 2) A region of thermal runaway and rapid temperature rise. Validations of homogeneous isobaric ignition temperature time histories are shown in Figure 2 for acetylene-air and ethylene-air systems, clearly showing excellent agreement with multi-step chemistry. In all these cases, the relevant equilibrium reaction rates and concentrations were calculated using the NASA CEA Equilibrium code [10].

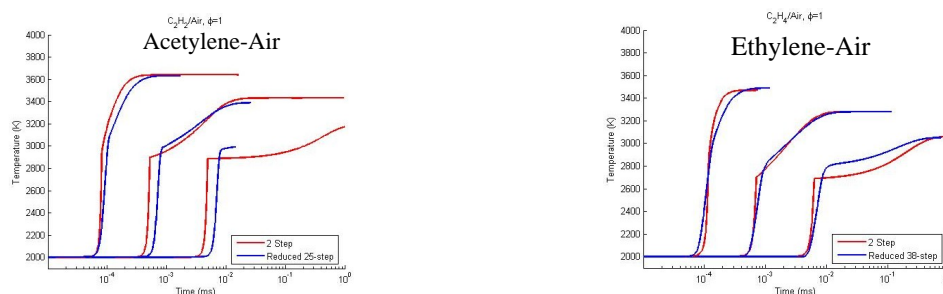


Figure 2: Homogeneous isobaric ignition temperature time histories using various mechanisms

(c) Turbulence model:

It is clear that the turbulence generated by obstacles and its interaction with chemistry are known to encourage flame acceleration and eventual DDT. In the present study, the standard k-epsilon was used to capture the turbulence effects. This turbulence model is robust, reasonably accurate and widely used in engineering computation. In this two-equation model, a very low turbulence intensity of 1% was used to initialize the flow field since a quiescent mixture inside the tube was assumed. The turbulence dissipation rate (ϵ) was calculated accordingly. Figure 3 shows the sensitivity studies of turbulence effects based on 3 different levels of initial turbulent viscosity. It should be noted that the initial turbulence dissipation rate had a significant effect on the subsequent simulated DDT process.

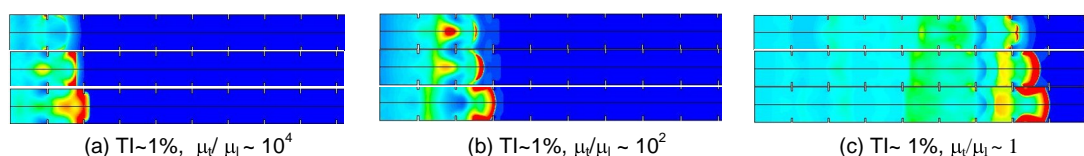


Figure 3: Turbulence effects study for detonation simulation: pressure contours at time instant of deflagration-to-detonation (if occurs) with different initial turbulent viscosity

(d). Thermal exchange and heat losses

The flame velocity at the beginning of the DDT process is low and the initial acceleration is linked to the “piston effect” of the hot gases. Therefore, heat loss due to heat transfer from flame to wall plays a prominent role in the DDT process. Experimentally, it is difficult to measure the amount of heat loss during the PDE test. The heat conduction model was incorporated in one of simulations to investigate the effect of heat loss on DDT at cold-start conditions. Figure 4 shows the comparison of the flame front for both adiabatic and thermal walls at three different time instants. The flame front shown at the first time instant, $t=41.4 \mu\text{s}$, represented the initial flame propagation stage in the DDT process. It clearly indicated that the flame is much smaller when heat loss is taken into account. At the second time instant, $t=85.6 \mu\text{s}$, the flame has transited into detonation in the adiabatic tube while the thermal tube took $130.1 \mu\text{s}$ for the deflagration to transit to detonation. The results also suggested a 5~10% increase in the simulated DDT distance when heat losses to the tube walls are taken into account.

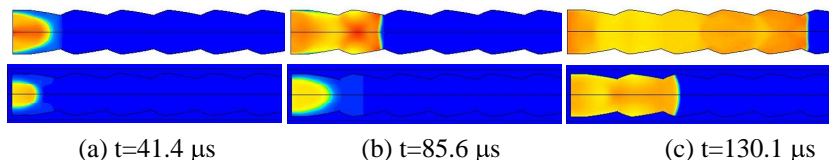


Figure 4: Simulated flame front at three time instants during DDT process for adiabatic (top row) and heat transfer (bottom row) models. (a) both are at deflagration; (b) DDT time for adiabatic tube; (c) DDT time for heat transfer tube.

From the preceding parametric studies of various CFD parameters including chemical kinetics and mesh size, key requirements for accurate CFD prediction of DDT process have been identified. For an ethylene-air mixture, a grid size of less than 0.25mm is required to reach grid convergent results. In the realm of chemical kinetics, a 2-step semi-empirical mechanism produced good results. This mechanism provided a cost-effective alternative to a detailed mechanism, and provides reasonable estimates when used in flame acceleration, SDT and DDT simulations. Heat transfer to the tube walls was also shown to have a profound effect on simulation results. The effects of initial turbulence distribution highlighted a potential source of discrepancy if the initial setup of the CFD model did not represent the initial flow conditions inside of the tube.

3 DDT computation and validation

All calculations were made using the FLUENT v6.2 CFD software package for finite volume calculations, with reactions accounted for via the 2-step mechanism implemented as a user-defined function (UDF). The

benchmark case used in the present CFD study was based on the experiment of de Witt *et al.* [11]. The tube internal diameter is 140mm, and the entire tube is 3.1m long. The first 1.36m of the tube is referred to as the flame acceleration section, and is filled with orifice plates equally spaced at 15.2cm. The blockage ratio of the plates is 0.42. The ignition of the initial deflagration is produced by a spark of energy 150mJ, and the tube is initially filled with a stoichiometric mixture of ethylene and air at 1 atm and 298K.

Simulations were carried out on 1-inch diameter obstacle-laden tubes with mesh size of 0.25mm using the two-step mechanism by Varatharajan [7]. The flame acceleration is monitored continuously throughout the propagation, and the velocity of the flame is recorded and compared with experimental data. The results were shown in Figure 5, with emphasis placed on the initial portion of the flame acceleration. When distances were scaled by the tube diameter, the initial flame acceleration (up to $x/D \sim 4$) profiles on the v - x plot for the large and small tubes (including experimental results) approximately collapse onto a single curve. This is consistent with experimental findings which suggest that, above a certain limit, the initial portions of the v - x' curve (where $x'=x/D$) roughly fall on top of each other for circular obstacle-laden tubes of similar geometry.

We can see from Figure 5 that the initial flame acceleration is fairly well predicted, albeit on the high side. In this experiment, it was found that the slow deflagration underwent transition into a choked flame, travelling at about half the CJ velocity, whereas the 2D CFD simulation showed a detonation at the CJ velocity. The comparison of CFD results conducted by Chapin *et al.* [12] indicated that the discrepancy between 2D axisymmetric and 3D simulations could be attributed to much smaller effects of irregular reflections and shock focusing effects in the case of 3D simulations when compared to 2D axisymmetric simulations. It is important to appreciate that the run-up distance is the only dynamic parameter for DDT which cannot be predicted *a priori* (Flame regimes are also dependent on thermodynamics as well as geometric parameters such as tube diameter). In other words, given a design which ensures transition to detonation, CFD can then be used to find the length required for such a transition to occur.

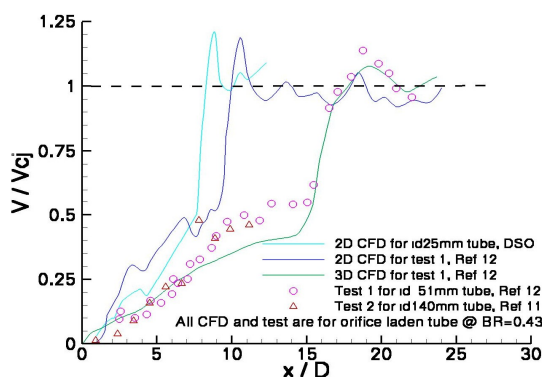


Figure 5: Flame acceleration against normalized downstream distance (CJ velocity = 1800 m/s).

4 Geometry effects

The presence of spirals and/or obstacles inside the detonation tube is known to be able to reduce the DDT distance. However, the use of spirals and/or obstacles usually introduces a drag penalty. Recently, I. Semenov *et al.* [13] proposed the use of a parabolic obstacle to promote the shock to detonation transition (SDT) process. When compared, simulations of orifice plates and parabolic obstacles as in Figure 6 showed that the latter achieved a considerable reduction of SDT distance and time. It is suggested in [13] that the physical mechanism governing the fast SDT is closely connected with explosive gas preconditioning by multiple shock compression in the vicinity of the focal points of the parabolic obstacles. As the parabolic obstacle may also offer lower drag penalty as compared to conventional obstacles such as spirals and orifice plates, a computational investigation of the effects of parabolic obstacles in the DDT process would thus be interesting.

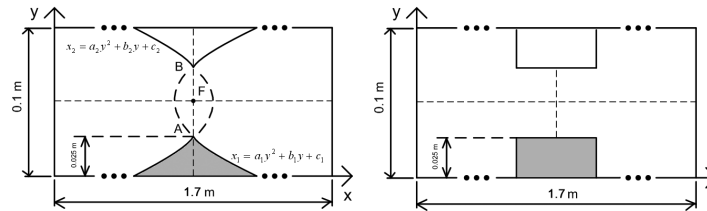


Figure 6: Schematic of parabolic shape obstacles and orifice obstacles (courtesy of I. Semenov and S. Frolov)

The first test case investigated was the SDT problem described in [13]. The main differences between the current work and that of [13] are that the initial work neglected turbulence effects, and used a single-step chemical kinetic mechanism for a propane/air mixture. In contrast, the present CFD study used a 2-step chemical kinetics for ethylene/air mixture with a standard k-ε turbulence model to account for turbulence effects. Figure 7 shows pressure and temperature contours at various time instants for a parabolic obstacle-laden channel. It can be seen that a ‘hot spot’ (area of high pressure and temperature) was created at the focal point near the 4th obstacle, which is consistent with the physical mechanism described by Semenov *et al.* as shown in Figure 8.

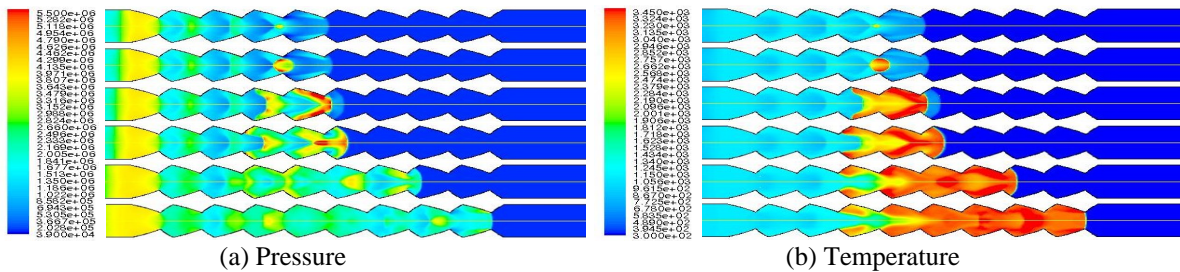


Figure 7: The simulated evolution processes of shock waves and flames for 2D SDT channel.

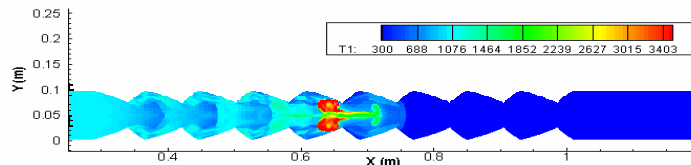


Figure 8: Snapshot of temperature fields in the channel with parabolic obstacle channel (courtesy of I. Semenov and S. Frolov)

Figure 9(a) shows the comparison of SDT distance for parabolic and orifice obstacles. The results indicate that parabolic obstacles could reduce the SDT distance and time as much as 30% when compared to orifice obstacles. It should be noted that in [13], detonation was not obtained in the case of the regular orifice plates where in scope of the present work SDT was observed in both cases (shaped obstacles and orifice plates).

The second test case was an axisymmetric domain using the same mesh as the 2D channel case. This, in turn, gave a blockage ratio of 75% as compared to the blockage ratio of 50% in the 2D channel model. Figure 9 shows the comparison of SDT distance with parabolic obstacles and orifice obstacles for both the 2D channel and axisymmetric configurations. It can be seen that the same physical mechanism controls the fast SDT process in the channel and axisymmetric simulations, and the reduction of SDT distance and time by parabolic obstacles reached as high as 60% as compared to the orifice obstacles in the axisymmetric simulation, possibly due to the much stronger shock wave compression caused by higher blockage ratio in the axisymmetric configuration.

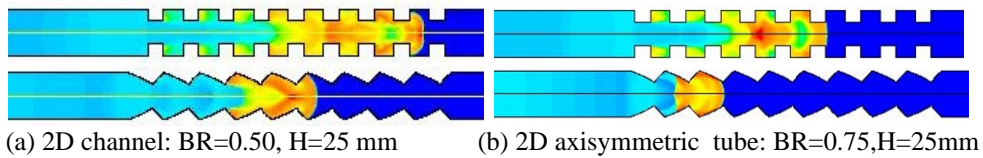
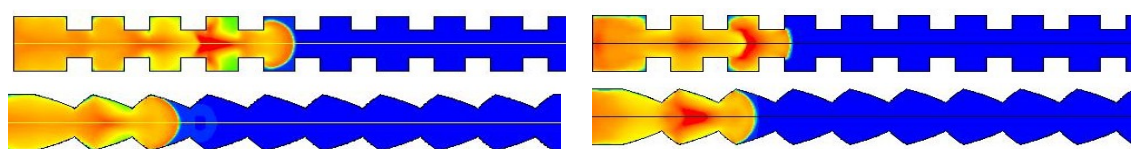


Figure 9: Comparison of SDT distance for 2D configuration: temperature contours.

The preceding results demonstrate the reduction of SDT distance and time by parabolic shaped obstacles with inclusion of turbulence effects and a 2-step kinetic model for ethylene/air mixture in the CFD simulations. Since the initial flame acceleration in a detonation tube is of critical importance in the design of PDE system, CFD simulations were carried out to investigate the effects of parabolic shaped obstacle geometries in the DDT process. All physical conditions were kept the same as the SDT cases but in the DDT cases, ignition was achieved with a point energy deposit of high pressure (5 MPa) and temperature (>8000 K) within a spark radius of 0.75 mm. Figure 10 showed the comparison of DDT distance for parabolic and orifice obstacles. The results indicated that parabolic obstacles could reduce the DDT distance and time as much as 50% when compared to orifice obstacles in 2D channel tube and up to 20% in axisymmetric tube. The compression and focusing of shock waves resulting from parabolic obstacles created hot spots and promoted transition to detonation. This further reduced the DDT distance and time as compared to the orifice obstacle-laden tube.

Compared to the SDT computation, the detonation was achieved closer to the ignition point, even with a lower blockage ratio. This is mostly caused by the choice of the ignition energy which caused an early coupling of the flame and shock-wave (near the second obstacle). Lower ignition energy generally leads to a much longer DDT distance.



(a) 2D channel: BR=0.50, H=25 mm (b) 2D axisymmetric tube: BR=0.75, H=25mm

Figure 10: Comparison of DDT distance for 2D configuration: temperature contours.

5 Conclusion

CFD studies of SDT and DDT have been performed to ascertain the effects of parabolic obstacles (*vis-à-vis* orifice plate obstacles) for the reduction of SDT and DDT distance and time. Other variables such as the effect of heat loss on the flame evolution of the DDT process at cold-start conditions were also investigated. In the realm of chemical kinetics, a 2-step semi-empirical mechanism was implemented and tested with good results. This mechanism provided a cost-effective alternative to a detailed mechanism, and provided reasonable estimates when used in flame acceleration, SDT and DDT simulations.

All essential phenomena related to flame acceleration, SDT and DDT have been captured computationally. These include the generation of hot spots behind a strengthening shock, shock/detonation wave reflection and diffraction, and the shortening of DDT distance due to the presence of obstacles. The results of the SDT and DDT simulations in an obstacle-laden tube showed that parabolic shaped obstacles could achieve a further reduction in DDT distance and time as compared to conventional orifice plate obstacles.

References

- [1] Shchelkin, K.I. (1949). Fast combustion and spinning detonation of gases. Moscow : Voenizdat 44-73
- [2] Chao, J., Kolbe, M., and Lee, J.H.S. (1999). Influence of tube and obstacle geometry on turbulent flame acceleration and deflagration to detonation transition. 17th ICDERS, Heidelberg, Germany
- [3] Vasil'ev, A.A. (2003). Optimization of accelerators of deflagration-to-detonation transition. in Confined Detonations and Pulse Detonation Engines, edited by G. Roy, S. Frolov, R. Santoro and S. Tsyganov, Moscow TORUS PRESS, 2003, ISBN 5-94588-012-4
- [4] Khokhlov, A.M., and Oran, E.S. (1999). Adaptive mesh numerical simulation of deflagration-to-detonation transition: the dynamics of hot spots. AIAA 99-3439

-
- [5] Kim, A., Anderson, D.A., Lu, F.K., and Wilson, D.R. (2000). Numerical simulation of transient combustion process in pulse detonation engine. AIAA 2000-0887
- [6] Mawid, M.A., Park, T.W., Sekar, B., and Arana, C. (1999). Numerical analysis of pulse detonation engines using global and reduced hydrocarbon kinetics. AIAA 99-4901
- [7] Varatharajan, B., Petrova, M., Williams, F.A., and Tanginala, V.E. (2005). Two-step chemical-kinetic descriptions for hydrocarbon-oxygen-diluent ignition and detonation applications. Proc. of the Combust. Inst., 30 (2005) 1869-1877.
- [8] Tanginala, V.E., Varatharajan, P.F., and Dean, A.J. (2004). Application of reduced mechanisms for PDE initiation. AIAA-2004-1209
- [9] Li, S.C., Varatharajan, B., and Williams, F.A. (2000). The chemistry of ethylene ignition for application to pulse detonation engines. AIAA-2000-3475
- [10] <http://www.grc.nasa.gov/WWW/CEAWeb>
- [11] de Witt, B., Ciccarelli, G., Zhang, F., and Murray, S. (2005). Shock reflection detonation initiation studies for pulse detonation engines. J. Propulsion Power, 21 (6) :117, 2005
- [12] Chapin, D. M., Tangirala, V. E., Rasheed, A., and Dean, A. J., Detonation Initiation in Moving Ethylene-Air Mixtures at Elevated Temperature and Pressure, AIAA 2006-4793 (2006)
- [13] Semenov, I., Frolov, S., Markov, V., and Utkin, P. (2006). Shock-to-detonation transition in tubes with shaped obstacles. in Pulsed and Continuous Detonations, edited by G. Roy, S. Frolov, and J. Sinibaldi, Moscow: TORUS PRESS, ISBN 5-94588-040-X